ACS Medicinal Chemistry Letters

pubs.acs.org/acsmedchemlett

Understanding Dermatan Sulfate−Heparin Cofactor II Interaction through Virtual Library Screening

Arjun Raghuraman, Philip D. Mosier, and Umesh R. Desai*

Department of Medicinal Chemistry and Institute for Structural Biology and Drug Discovery, Virginia Commonwealth University, Richmond, Virginia 23298-0540

ABSTRACT Dermatan sulfate, an important member of the glycosaminoglycan family, interacts with heparin cofactor II, a member of the serpin family of proteins, to modulate antithrombotic response. Yet, the nature of this interaction remains poorly understood at a molecular level. We report the genetic algorithm-based combinatorial virtual library screening study of a natural, high-affinity dermatan sulfate hexasaccharide with heparin cofactor II. Of the 192 topologies possible for the hexasaccharide, only 16 satisfied the "high-specificity" criteria used in computational study. Of these, 13 topologies were predicted to bind in the heparin-binding site of heparin cofactor II at a ~60° angle to helix D, a novel binding mode. This new binding geometry satisfies all known solution and mutagenesis data and supports thrombin ternary complexation through a template mechanism. The study is expected to facilitate the design of allosteric agonists of heparin cofactor II as antithrombotic agents.

KEYWORDS Computational biology, dermatan sulfate, glycosaminoglycans, heparin cofactor II, serpins, structure−activity relationships

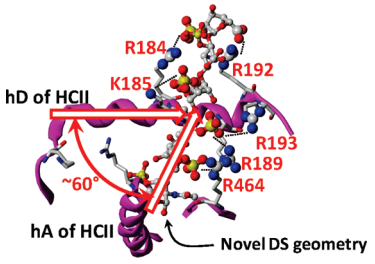

Glycosaminoglycans (GAGs) play critical roles in a number of physiological and pathological processes such as hemostasis, inflammation, neural growth, angiogenesis, and viral invasion. These roles arise from their interaction with a multitude of proteins. Yet, the structural elements that induce these interactions remain elusive, except perhaps for the heparin−antithrombin (AT) interaction.[1−3]

A fundamental reason for this poor understanding is their phenomenal structural diversity. GAGs are anionic copolymers of glycosamine and uronic acid residues, which are variously modified through sulfation, acetylation, and epimerization. Added to these variations are the multiple helical structures adopted by polymeric GAG chains. For example, dermatan sulfate (DS) can assume either 2_1-, 3_2-, or 8_3-fold helix.[4] Further compounding the structural diversity is conformational flexibility of the constituent residues. For example, iduronic acid (IdoA*p*), a residue present in DS and heparin, exhibits four major conformers: $^1C_4$, $^4C_1$, ^2S_O, and $^OS_2$.[5,6] This combination of configurational and conformational variations leads to an exponential number of GAG topologies. A simple calculation reveals that 884736 different topologies are possible for a DS hexasaccharide, of which a select few may induce a physiological response.

A potentially powerful approach to address GAG−protein interactions is computational analysis. Yet, modeling GAGs has been problematic due in part to their polyanionic nature and poor surface complementarity.[7,8] Recently, we developed a combinatorial virtual library screening (CVLS) approach using the genetic algorithm-based automated docking program GOLD and a library of 6859 heparin hexasaccharide sequences.[9] Application of the CVLS methodology to heparin recognition of AT resulted in the identification of several putative "high-affinity and high-specificity" heparin sequences as well as an accurately predicted description of the binding mode of the heparin pentasaccharide H5 (Figure 1) consistent with experimentally determined H5−AT structure−activity relationships. The success of this approach for the heparin−AT interaction pair suggests its possible use for its sister pair, the DS−heparin cofactor II (HCII) system, which remains structurally undefined and less well-understood at a molecular level.

The DS−HCII system has a number of important physiological roles.[10−13] HCII is a human plasma serine proteinase inhibitor (serpin) that specifically inhibits thrombin,[14] a key enzyme playing a critical role in hemostasis. The intrinsic specificity of HCII may be a unique advantage because its deficiency does not appear to enhance risk for thrombosis.[15] At the same time, the serpin prevents arterial thrombosis.[11,12,15,16] HCII is also able to inhibit clot-bound thrombin, in striking contrast to AT.[17] Despite these advantages, no anticoagulant has yet been developed that utilizes the HCII-based indirect pathway of coagulation regulation.

Received Date: March 6, 2010
Accepted Date: June 6, 2010
Published on Web Date: June 14, 2010

DOI: 10.1021/ml100048y | *ACS Med. Chem. Lett.* **2010**, *1*, 281–285

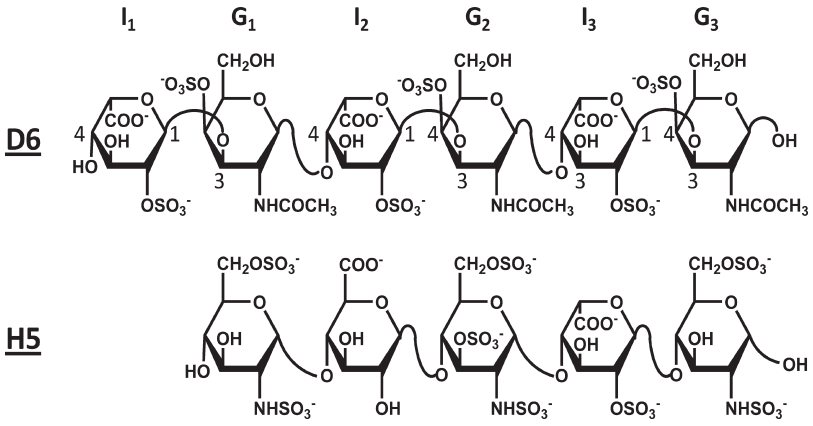

Figure 1. Structures of dermatan sulfate hexasaccharide D6, which is known to bind to HCII, and H5, which is known to bind to AT.

The inhibition of thrombin by HCII is accelerated nearly 1000-fold in the presence of DS. A rare DS hexasaccharide D6 (Figure 1) has been shown to bind HCII with high affinity, while DS sequences with higher levels of sulfation bind poorly, suggesting significant specificity of interaction.[18,19] On a three-dimensional level, HCII is structurally similar to AT. For example, Lys114, Lys125, and Arg129, the three key heparin-binding residues in AT, correspond to Lys173, Lys185, and Arg189 of helix D in HCII. Likewise, Arg46, Arg47, Arg132, and Lys133 of AT match Lys101, Arg103, Arg192, and Arg193 of HCII. Yet, H5 (Figure 1), which recognizes AT with high affinity and high specificity, binds HCII poorly.[20] On the other hand, it is known that DS does not interact with Arg103 and Lys173,[21,22] as one would expect on the basis of the structural similarity of AT and HCII. Overall, despite the availability of much biochemical data, the structure of the DS−HCII complex remains unknown and unexploited.

In this work, we predict the HCII binding geometry of the high-affinity DS hexasaccharide D6 using the CVLS approach that we developed earlier.[9] To assess how D6 might interact with HCII, we sought to prepare all possible topologies of the hexasaccharide. Thus, using three possible helical folds (2_1-, 3_2-, or 8_3-helices), four possible major conformers ($^1C_4$, $^4C_1$, ^2S_O, and $^OS_2$) for IdoA*p*, and the most favored conformer for galactosamine residue (GalN*p*) ($^4C_1$), 192 topologies ($3 \times 4 \times 4 \times 4$) were generated for D6 in a combinatorial manner with SYBYL using in-house Sybyl Programming Language (SPL) scripts. The crystal structure of the activated form of HCII was extracted from the S195A thrombin−HCII Michaelis complex (PDB entry 1JMO),[23] which is similar to that of activated AT.[24,25] Because of its high degree of similarity to the heparin binding site in AT and site-directed mutagenesis studies, the region formed by helices A and D was predicted to be the binding site for D6 in HCII.

Our CVLS approach to understand the interaction of D6 with HCII utilized a variation of the dual-filter docking and scoring strategy tailored for the study of GAG−protein interactions (Figure 2).[9] In this strategy, GOLD was used to sample possible interaction poses and assess their fitness

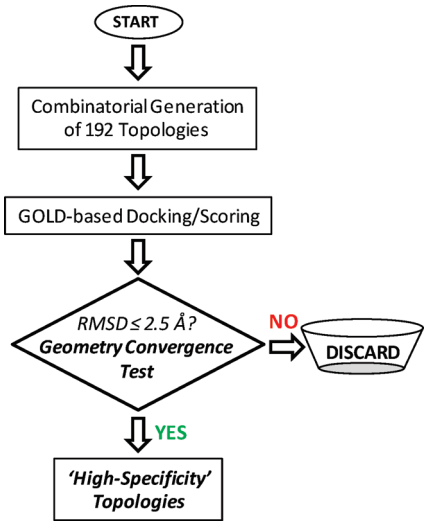

Figure 2. CVLS algorithm used to study the interaction of 192 D6 topologies with HCII.

to the GOLDScore function. GOLD utilizes a genetic algorithmic search in which an initial population of 100 randomly docked D6 orientations for each topology is evaluated by the scoring function and iteratively improved through a bias for higher scores. The top-ranked solutions for each topology were then subjected to a "specificity" filter in which self-consistency of docking, when performed multiple times, was assessed. The top two solutions from three independent docking runs (six solutions total) were compared. D6 topologies that had a rmsd among the six solutions of less than 2.5 Å were deemed to be geometries that recognize HCII highly consistently. Such D6 topologies were considered as "high-specificity" topologies. A detailed description of the protocol employed is provided in the Supporting Information.

Of the 192 D6 topologies that were subjected to the CVLS analysis, only 16 satisfied the criterion of "high specificity". Table S1 (see Supporting Information) describes the interactions of the 16 topologies of D6 with key amino acid residues of helices A and D in HCII. The compilation reveals several striking features. Of the 64 possible 8_3-helix topologies in the

DOI: 10.1021/ml100048y | *ACS Med. Chem. Lett.* **2010**, *1*, 281–285

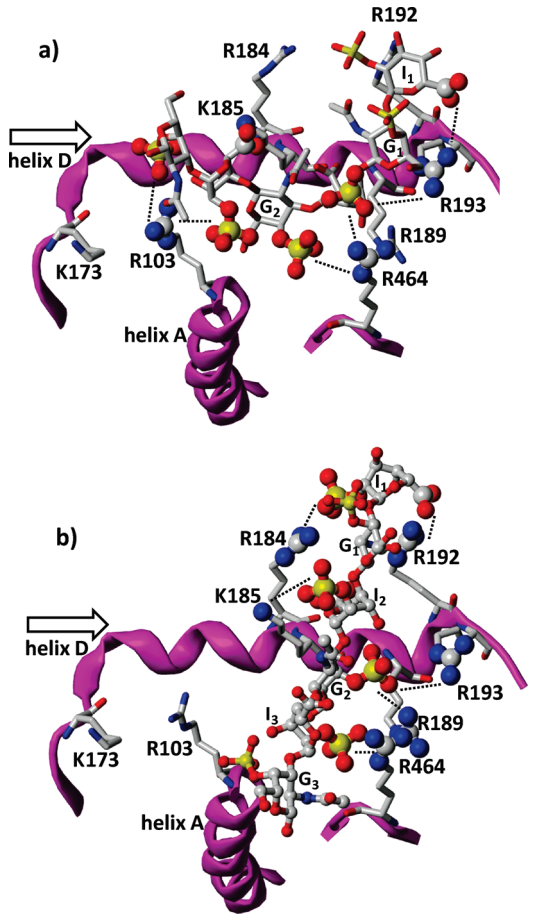

Figure 3. Putative binding modes of two D6 topologies with HCII. Helices D and A are shown in magenta. Basic residues of HCII are shown as sticks, and the D6 sequence is rendered as ball-and-stick. (a) A representative parallel binding topology, 3_2-$^{2}S_O\cdot{}^{O}S_2\cdot{}^{1}C_4$. (b) Skewed (~60°) binding "hit" topology 2_1-$^{O}S_2\cdot{}^{1}C_4\cdot{}^{1}C_4$. Amino acid, sulfate, and carboxylate atoms involved in putative D6–HCII interactions are highlighted by using an increased van der Waals radius. Interactions among these functional groups are indicated using dotted lines. Labels I_1–I_3 and G_1–G_3 are saccharide residue labels (see Figure 1). The direction of the helix D axis is shown by an arrow. Stereoviews of both binding modes are available in the Supporting Information (Figure S2).

library, none docked with "high specificity". Of the remaining 128 topologies, two 2_1- and 14 3_2-helices satisfied the criterion. The binding modes of these 16 "high-specificity" topologies could be segregated into two major families. The first mode of binding is parallel to helix D (Figure 3a), a mode nearly identical to that of H5 binding to AT.[24,25] The second family of D6 topologies interacts with helix D at an angle of roughly 60° (Figure 3b). Only three topologies fall in the first family, while 13 comprise the latter.

The D6 topologies that dock parallel to helix D do not interact with Arg189 and Arg193, two of the five residues found important for binding DS.[26−28] At the same time, they engage Arg103, which is known not to play a role in the DS–HCII interaction.[21,29] Thus, these three topologies were ruled out. Of the 13 topologies that bound at ~60° angle to helix D, two had a 2_1-fold helical geometry, while the rest were 3_2-fold helices. The orientation of each of these topologies is similar and interacts strongly with two critical DS binding residues: Arg184 and Arg189.[26] Yet, significant differences arise in interactions of these topologies with other residues of helices A and D. None of the 3_2-helix topologies interact with Lys185, which is known to be an important residue for DS recognition.[21] Furthermore, at least five 3_2-helix topologies interact with Arg103, a residue known to be not involved in DS binding.[21,29] Thus, the 11 3_2-helix topologies were ruled out.

This leaves only two 2_1-helix topologies as possible HCII binding geometries. Of these two, only one, that is, 2_1-$^{O}S_2\cdot{}^{1}C_4\cdot{}^{1}C_4$, interacts with all five key amino acid residues known to be involved in binding to HCII (Figure 3b), while not interacting with Arg103 and Lys173, which are known to be not involved in HCII recognition (see Table S1 in Supporting Information). The 2_1-$^{O}S_2\cdot{}^{1}C_4\cdot{}^{1}C_4$ topology satisfies all of the known biochemical data. This binding geometry, exhibiting a ~60° angle with helix D, is radically different from that of pentasaccharide H5 binding to AT, despite a strong degree of structural and sequence similarity between the two serpins.

A key question to address at this point is whether rotameric states of the amino acid residues, especially the positively charged Lys and Arg implicated in binding, are likely to affect the outcome of the computational study. A priori, the surface-exposed Lys and Arg residues are likely to exhibit multiple rotameric states; however, the majority of HCII residues that strongly interact with the 2_1-$^{O}S_2\cdot{}^{1}C_4\cdot{}^{1}C_4$ topology show an extended side chain conformation, which is the preferred form because of steric and/or electrostatic forces arising from neighboring residues. This conformational restriction introduced by neighboring residues appears to be an important reason for the preferential recognition of the 2_1-$^{O}S_2\cdot{}^{1}C_4\cdot{}^{1}C_4$ topology. The residues that are known to not interact with DS also show a similar characteristic. Arg103 is held in place by a hydrophobic groove formed by neighboring residues that restrict its conformational flexibility, while Lys173 is so far away that its side chain flexibility will not play any role. Thus, the conformational states of the side chains constituting the DS binding site are unlikely to drastically change the outcome of the CVLS study.

Support for the validity of the "hit" 2_1-$^{O}S_2\cdot{}^{1}C_4\cdot{}^{1}C_4$ topology is provided by conformational studies of DS in solution. For example, Scott et al. report that DS adopts a 2-fold helical conformation in solution using NOE spectroscopy.[30] Likewise, Silipo et al. report on the use of NMR and molecular modeling study to show that a DS tetrasaccharide, very similar to D6, exists as four major species in solution, of which two have a 2-fold helical conformation.[31] Additionally, the GalN*p*N2Ac4S and IdoA*p* residues of this DS tetrasaccharide possess $^{4}C_1$ and $^{1}C_4$ conformations, respectively, which are similar to the conformations of the residues present in the "hit" D6 topology.[31]

Another key test of the novel D6 binding geometry is whether it supports bridged ternary complexation with thrombin, an important mechanism of DS activation of HCII.[32] Overlaying D6 in the novel binding geometry (~60° to helix D) onto the HCII–T cocrystal structure (PDB code 1JMO[23]) shows that D6

DOI: 10.1021/ml100048y | *ACS Med. Chem. Lett.* **2010**, *1*, 281–285

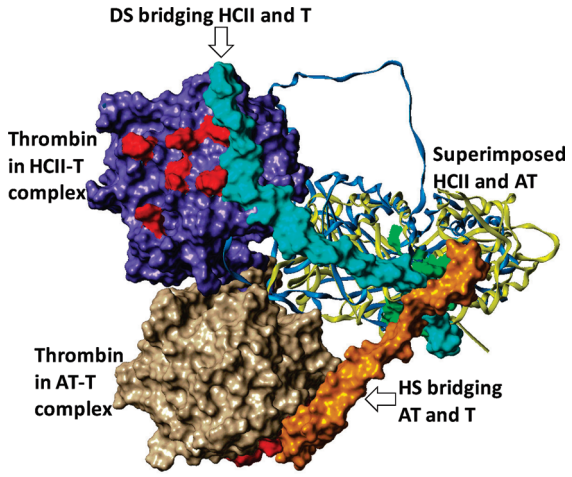

Figure 4. Comparison of GAG-bridged ternary complexes formed by AT−T (yellow ribbon and tan and orange surfaces; PDB code 1TB6) and HCII−T (blue ribbon and purple surface; PDB code 1JMO). The two serpins, AT and HCII, of the two complexes were aligned. 1TB6 also contains the GAG (heparin-like). The DS GAG chain shown in this figure was modeled by extending the 2_1-$^{O}S_2 \cdot {}^{1}C_4 \cdot {}^{1}C_4$ D6 geometry by nine disaccharide units (cyan surface, IdoA*p*2S conformation = $^{2}S_O$). The relative orientation of T and its exosite II (basic residues shown in red) relative to the aligned heparin binding sites (green surfaces; partially occluded) is different in the two systems. See the text for details.

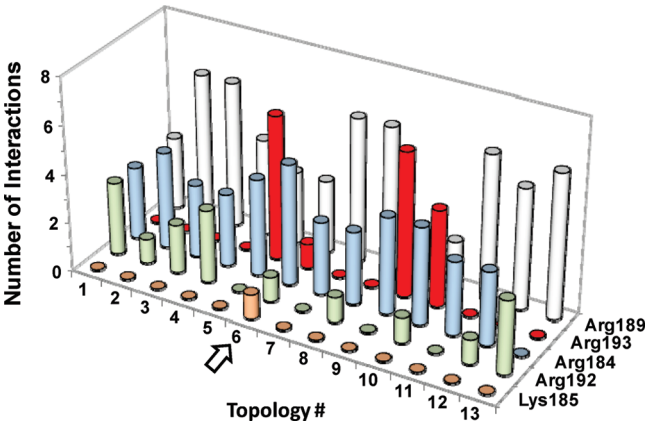

Figure 5. Profile of interactions made by 13 D6 topologies that bind HCII at ~60° to helix D. The level of interaction between D6 and an amino acid residue was determined by the number of unique interatomic distances that are less than 4.0 Å between the nitrogen atom(s) of the basic side chain and the sulfate or carboxylate oxygen atoms of D6 [see the Supporting Information (Figure S1) for a representative example of this interaction]. Interactions made by Arg464 and Arg 103 as well as those made by three topologies that bind parallel to helix D are not shown for clarity. The arrow highlights topology #6 (2_1-$^{O}S_2 \cdot {}^{1}C_4 \cdot {}^{1}C_4$, see Table S1 in Supporting Information), which was the only topology found to interact with all amino acid residues important for DS binding as well as not interact with Arg103. See the text for details.

is oriented in the direction of thrombin (Figure 4). When the D6 sequence was extended by nine disaccharides, in which all IdoA*p* residues are in the $^{2}S_O$ conformation, the DS oligosaccharide chain was found to intersect with exosite II of thrombin at Arg93, Arg101, and Lys240 (Figure 4).

Exosite II of thrombin is a well-studied GAG-binding domain that contributes greatly to HCII as well as AT inhibition of thrombin through the bridging mechanism.[2,32] Comparison of the AT−T and HCII−T cocrystal structures shows that although the serpins are strikingly similar, the position of thrombin in the two is dramatically different (Figure 4). In addition, the orientation of exosite II is also different. The distance between centrally located thrombin exosite II residue Arg233 and Lys125 in the AT−T system is about 55 Å, while the corresponding distance between Arg233 and Lys185 in the HCII−T system is about 70 Å. Therefore, while a GAG chain parallel to helix D of AT would engage exosite II in thrombin, the same chain oriented parallel of helix D of HCII would completely miss thrombin (Figure 4). In essence, this analysis strongly supports a novel 60° to helix D binding geometry of D6 onto HCII.

Several aspects of the "hit" D6 binding geometry are interesting. In this geometry, all of the 2-OSO_3^- groups of the IdoA*p*2S residues (Figure 1) interact strongly with HCII, suggesting a broad interaction interface. It is known that 2-*O*-sulfated IdoA*p* residues are uncommon in DS GAGs. Three successive IdoAp2S residues are even more so.[18,19,33] The extensive interactions of this rare sequence explain why common DS−GAG sequences (with unsulfated IdoA*p*) are inactive and support the idea that the hexasaccharide D6−HCII interaction is specific. In addition, the skewed ~60° binding geometry also implicates the 4-OSO_3^- group of D ring and the 6-COO^- group of ring A to have strong interactions with HCII (Figure 5). In vivo studies in HCII-deficient mice suggest that Gal*p*N2Ac4S is important for HCII-dependent antithrombotic effect,[13] thus lending support to this conclusion. The results lead to a hypothesis that D6 variants devoid of the two key groups (4-OSO_3^- of D and 6-COO^- of ring A) are likely to recognize HCII with weak or poor affinity.

The binding geometry implicates Arg464, a hitherto unheralded residue, as being important for D6 recognition. Our results suggest that Arg464 is capable of recognizing D6 in all 16 topologies (Figure 5). It is the first time that Arg464 has been implicated in specific recognition of DS and provides a firm hypothesis for testing the CVLS-derived binding geometry. Biochemical studies with a Arg464 mutant HCII could be performed to verify its involvement in the recognition of D6 and DS.

In summary, our combinatorial virtual screening procedure has identified a novel binding geometry for a rare DS sequence that binds HCII with high affinity. The results suggest that this binding is specific. The novel binding geometry (~60° angle to helix D) supports thrombin binding to HCII through a template mechanism. This is the first application of combinatorial virtual screening for DS−GAGs and affords extraction of a "pharmacophore" involved in DS−HCII interaction, which will greatly aid rational design of agonists and/or antagonists directed toward HCII. Finally, our approach is expected to be generally useful for other GAG−serpin interactions.

SUPPORTING INFORMATION AVAILABLE Computational experimental procedures and Table S1. This material is available free of charge via the Internet at http://pubs.acs.org.

DOI: 10.1021/ml100048y | *ACS Med. Chem. Lett.* **2010**, *1*, 281–285

AUTHOR INFORMATION

Corresponding Author: *To whom correspondence should be addressed. Tel: 804-828 7328. Fax: 804-827 3664. E-mail: urdesai@vcu.edu.

Funding Sources: This work was supported by NHLBI Grants HL090782 and HL099420, AHA Grant 0640053N, and the Mizutani Foundation for Glycoscience.

REFERENCES

(1) Capila, I.; Linhardt, R. J. Heparin−Protein Interactions. *Angew. Chem., Int. Ed. Engl.* **2002,** *41*, 391–412.
(2) Desai, U. R. New Antithrombin-Based Anticoagulants. *Med. Res. Rev.* **2004,** *24*, 151–181.
(3) Gandhi, N. S.; Mancera, R. L. The Structure of Glycosaminoglycans and Their Interactions with Proteins. *Chem. Biol. Drug Des.* **2008,** *72*, 455–482.
(4) Mitra, A. K.; Arnott, S.; Atkins, E. D. T.; Isaac, D. H. Dermatan Sulfate: Molecular Conformations and Interactions in the Condensed State. *J. Mol. Biol.* **1983,** *169*, 873–901.
(5) Ragazzi, M.; Ferro, D. R.; Provasoli, A. A. Force-Field Study of the Conformational Characteristics of the Iduronate Ring. *J. Comput. Chem.* **1986,** *7*, 105–112.
(6) Venkataraman, G.; Sasisekharan, V.; Cooney, C. L.; Langer, R.; Sasisekharan, R. A. Stereochemical Approach to Pyranose Ring Flexibility: Its Implications for the Conformation of Dermatan Sulfate. *Proc. Natl. Acad. Sci. U.S.A.* **1994,** *91*, 6171–6175.
(7) Grootenhuis, P. D. J.; van Boeckel, C. A. A. Constructing a Molecular Model of the Interaction Between Antithrombin III and a Potent Heparin Analog. *J. Am. Chem. Soc.* **1991,** *113*, 2743–2747.
(8) Bitomsky, W.; Wade, R. C. Docking of Glycosaminoglycans to Heparin-Binding Proteins: Validation for aFGF, bFGF, and Antithrombin and Application to IL-8. *J. Am. Chem. Soc.* **1999,** *121*, 3004–3013.
(9) Raghuraman, A.; Mosier, P. D.; Desai, U. R. Finding Needle in a Haystack. Development of a Combinatorial Virtual Screening Approach for Identifying High Specificity Heparin/Heparan Sulfate Sequence(s). *J. Med. Chem.* **2006,** *49*, 3553–3562.
(10) Weitz, J. I.; Hudoba, M.; Massel, D.; Maraganore, J.; Hirsh, J. Clot−Bound Thrombin is Protected from Inhibition by Heparin-Antithrombin III but is Susceptible to Inactivation by Antithrombin III−Independent Inhibitors. *J. Clin. Invest.* **1990,** *86*, 385–391.
(11) He, L.; Vicente, C. P.; Westrick, R. J.; Eitzman, D. T.; Tollefsen, D. M. Heparin Cofactor II Inhibits Arterial Thrombosis after Endothelial Injury. *J. Clin. Invest.* **2002,** *109*, 213–219.
(12) Aihara, K.-I.; Azuma, H.; Takamori, N.; Kanagawa, Y.; Akaike, M.; Fujimura, M.; Yoshida, T.; Hashizume, S.; Kato, M.; Yamaguchi, H.; Kato, S.; Ikeda, Y.; Arase, T.; Kondo, A.; Matsumoto, T. Heparin Cofactor II is a Novel Protective Factor Against Carotid Atherosclerosis in Elderly Individuals. *Circulation* **2004,** *109*, 2761–2765.
(13) Vicente, C. P.; He, L.; Pavão, M. S. G.; Tollefsen, D. M. Antithrombotic Activity of Dermatan Sulfate in Heparin Cofactor II-Deficient Mice. *Blood* **2004,** *104*, 3965–3970.
(14) Tollefsen, D. M. Heparin Cofactor II. *Adv. Exp. Med. Biol.* **1997,** *425*, 35–44.
(15) Tollefsen, D. M. Heparin Cofactor II Deficiency. *Arch. Pathol. Lab. Med.* **2002,** *126*, 1394–1400.
(16) Takamori, N.; Azuma, H.; Kato, M.; Hashizume, S.; Aihara, K.-I; Akaike, M.; Tamura, K.; Matsumoto, T. High Plasma Heparin Cofactor II Activity is Associated with Reduced Incidence of In-Stent Restenosis After Percutaneous Coronary Intervention. *Circulation* **2004,** *109*, 481–486.
(17) Bendayan, P.; Boccalon, H.; Dupouy, D.; Boneu, B. Dermatan Sulfate is a More Potent Inhibitor of Clot-Bound Thrombin than Unfractionated and Low Molecular Weight Heparins. *Thromb. Haemostasis* **1994,** *71*, 576–580.
(18) Maimone, M. M.; Tollefsen, D. M. Structure of a Dermatan Sulfate Hexasaccharide that Binds to Heparin Cofactor II with High Affinity. *J. Biol. Chem.* **1990,** *265*, 18263–18271.
(19) Pavão, M. S.; Mourão, P. A.; Mulloy, B.; Tollefsen, D. M. A Unique Dermatan Sulfate-like Glycosaminoglycan from Ascidian. Its Structure and the Effect of its Unusual Sulfation Pattern on Anticoagulant Activity. *J. Biol. Chem.* **1995,** *270*, 31027–31036.
(20) Maimone, M. M.; Tollefsen, D. M. Activation of Heparin Cofactor II by Heparin Oligosaccharides. *Biochem. Biophys. Res. Commun.* **1988,** *152*, 1056–1061.
(21) Blinder, M. A.; Tollefsen, D. M. Site-Directed Mutagenesis of Arginine 103 and Lysine 185 in the Proposed Glycosaminoglycan-Binding Site of Heparin Cofactor II. *J. Biol. Chem.* **1990,** *265*, 286–291.
(22) Whinna, H. C.; Blinder, M. A.; Szewczyk, M.; Tollefsen, D. M.; Church, F. C. Role of Lysine 173 in Heparin Binding to Heparin Cofactor II. *J. Biol. Chem.* **1991,** *266*, 8129–8135.
(23) Baglin, T. P.; Carrell, R. W.; Church, F. C.; Esmon, C. T.; Huntington, J. A. Crystal Structures of Native and Thrombin-Complexed Heparin Cofactor II Reveal a Multistep Allosteric Mechanism. *Proc. Natl. Acad. Sci. U.S.A.* **2002,** *99*, 11079–11084.
(24) Jin, L.; Abrahams, J. P.; Skinner, R.; Petitou, M.; Pike, R. N.; Carrell, R. W. The Anticoagulant Activation of Antithrombin by Heparin. *Proc. Natl. Acad. Sci. U.S.A.* **1997,** *94*, 14683–14688.
(25) Li, W.; Johnson, D. J. D.; Esmon, C. T.; Huntington, J. A. Structure of the Antithrombin-Thrombin-Heparin Ternary Complex Reveals the Antithrombotic Mechanism of Heparin. *Nat. Struct. Mol. Biol.* **2004,** *11*, 857–862.
(26) Blinder, M. A.; Andersson, T. R.; Abildgaard, U.; Tollefsen, D. M. Heparin Cofactor II_{Oslo}. Mutation of Arg-189 to His Decreases the Affinity for Dermatan Sulfate. *J. Biol. Chem.* **1989,** *264*, 5128–5133.
(27) Liaw, P. C. Y.; Austin, R. C.; Fredenburgh, J. C.; Stafford, A. R.; Weitz, J. I. Comparison of Heparin- and Dermatan Sulfate-Mediated Catalysis of Thrombin Inactivation by Heparin Cofactor II. *J. Biol. Chem.* **1999,** *274*, 27597–27604.
(28) He, L.; Giri, T. K.; Vicente, C. P.; Tollefsen, D. M. Vascular Dermatan Sulfate Regulates the Antithrombotic Activity of Heparin Cofactor II. *Blood* **2008,** *111*, 4118–4125.
(29) Hayakawa, Y.; Hirashima, Y.; Kurimoto, M.; Hayashi, N.; Hamada, H.; Kuwayama, N.; Endo, S. Contribution of Basic Residues of the A Helix of Heparin Cofactor II to Heparin- or Dermatan Sulfate-Mediated Thrombin Inhibition. *FEBS Lett.* **2002,** *522*, 147–150.
(30) Scott, J. E.; Heatley, F.; Wood, B. Comparison of Secondary Structures in Water of Chondroitin-4-Sulfate and Dermatan Sulfate: Implications in the Formation of Tertiary Structures. *Biochemistry* **1995,** *34*, 15467–15474.
(31) Silipo, A.; Zhang, Z.; Cañada, F. J.; Molinaro, A.; Linhardt, R. J.; Jiménez-Barbero, J. Conformational Analysis of a Dermatan Sulfate-Derived Tetrasaccharide by NMR, Molecular Modeling, and Residual Dipolar Couplings. *ChemBioChem* **2008,** *9*, 240–252.
(32) Verhamme, I. M.; Bock, P. E.; Jackson, C. M. The Preferred Pathway of Glycosaminoglycan-Accelerated Inactivation of Thrombin by Heparin Cofactor II. *J. Biol. Chem.* **2004,** *279*, 9785–9795.
(33) Tollefsen, D. M. The Interaction of Glycosaminoglycans with Heparin Cofactor II: Structure and Activity of a High-Affinity Dermatan Sulfate Hexasaccharide. *Adv. Exp. Med. Biol.* **1992,** *313*, 167–176.

DOI: 10.1021/ml100048y | *ACS Med. Chem. Lett.* **2010,** *1*, 281–285